Lithosphere

Research Article

The Statistical Damage Constitutive Model of Longmaxi Shale under High Temperature and High Pressure

Qinyou Ye,[1,2] **Xujiao He,**[3] **Yu Suo** ⓘ **,**[1,4] **Sicong Zhao,**[5] **Chi Ai,**[1] **Lei Qiao,**[6] **Minggu Song,**[7] **Xiling Chen,**[8] **and XiaoJin Zhou**[9]

[1]*School of Petroleum Engineering, Northeast Petroleum University, Daqing, China*
[2]*Unconventional Resources Development Company of PetroChina Jilin Oilfield Company, Songyuan, China*
[3]*Research Institute of Petroleum Exploration & Development, Beijing, China*
[4]*Postdoctoral Resource Centre, Daqing Oilfield Company Limited, Daqing, China*
[5]*Tenth Oil Production Plant of Daqing, Daqing Oilfield Company Limited, Daqing, China*
[6]*CNPC Engineering Technology R & D Company Limited, Beijing, China*
[7]*Second Oil Production Plant of Daqing, Daqing Oilfield Company Limited, Daqing, China*
[8]*Liaohe Oilfield Petroleum Exploration & Development Research Institute, Panjin, China*
[9]*Shale Gas Research Institute, PetroChina Southwest Oil & Gas Field Company, Chengdu, China*

Correspondence should be addressed to Yu Suo; sycup09@163.com

In the exploitation of shale gas in deep and ultradeep formations, the mechanical properties of shale change under the action of high temperature and pressure. High-temperature stimulation can effectively release the damage of water phase trapping, which was caused during the drilling and completion of hydraulic fracturing of shale gas reservoirs. In this paper, the experiments have twelve groups of shale samples (three samples per group) under four target temperatures, 25, 200, 400, and 600°C as well as the confining pressure set as 0 MPa, 15 MPa, and 30 MPa. The servo testing machine is used to perform triaxial compression tests on the shale specimens that have undergone high temperature. The porosity, permeability, and velocity are also obtained under different temperatures. A statistical constitutive model of shale after temperature thermal damage under triaxial compression is established. Based on the characteristics of the random statistical distribution of rock strength and strain strength theory, apply relevant knowledge of damage mechanics as well as consider the failure of the microprotocol and the nonlinear relationship between elastic modulus and temperature. According to the test results, the relationship between the mechanical parameters of the shale and the temperature is discussed. The parameters of the statistical constitutive model considering temperature thermal damage are given also; a comparison with the results of uniaxial compression experiments shows the rationality and reliability. This work not only enriches the theory of shale failure pattern but also contributes to the deep shale development at high temperature.

1. Introduction

In recent years, the development of unconventional energy such as shale gas reservoirs has gradually entered people's vision with the continuous improvement of underground exploration technology. The large-scale development and utilization of shale gas play a positive role in improving national energy security, reducing external dependence on energy, and alleviating the shortage of natural gas supply.

With the reservoir depth increase, the mechanical properties and temperature around the shale change a lot. It is extremely significant to guarantee the stability and safety of rock engineering under high temperature, such as the on-site gasification of coal and oil shale, underground mining, and storage of oil and natural gas [1]. As the temperature of shale reservoir increases, the pore structure of shale is changed and it is necessary to clarify the changes in the shale's physical and mechanical properties with increasing

temperature. Also, the stress-strain relationship of shale will change undergo high-temperature and confining pressure conditions. The method to increase the reservoir temperature can also promote the desorption of shale gas and speed up the development of shale gas reservoirs.

The damage mechanics was first put forward by Kachannov [2] and later introduced into the field of rock mechanics by Dougill [3]. It has become an important theory for studying rock damage and has made some breakthroughs in rock damage mechanics. For instance, the rock constitutive model based on damage mechanics has been used in stress and strain analysis of materials in geotechnical engineering design. The stress-strain relationship will change after the shale undergoes high-temperature treatment and high pressure. It shows that there is an inseparable connection between the constitutive model of shale and temperature by researchers. Gambarotta and Lagomarsino [4] established a damage model of brittle materials under arbitrary stress by considering the sparse distribution of planar microcracks. Yu and Feng [5] established a three-dimensional damage model of brittle materials with microcracks based on damage mechanics theory and defined the crack propagation area as all possible paths and directions of microcracks after loading. Zhou et al. [6] adopted the homogenization method and based on rock damage mechanics to assuming that the microcracks follow a random distribution. The brittle rock under uniaxial compression with microcrack damage model was proposed. Hamdi et al. [7] used digital imaging technology to quantify the rock damage problem in the core and defined the internal damage of the rock as the ratio between the crack area and the total image area. On this basis, a tensile damage model of limestone was established. Li and Tang [8] established the process of rock's cross-scale progressive failure of rock mesodamage mechanical method. The mesoconstitutive equation of RVE is established, and the mesoanisotropy of rock materials is described by statistical methods. The stress field and strain field were solved using the finite element method. Huang et al. [9] proposed a new statistical damage constitutive model which consider freeze-thaw and loading; at the same time, it can be applied to coupled freeze-hydromechanical condition. Bian et al. [10] carried out to establish the constitutive model for shale regarding immersion time and uniaxial loading. Shen et al. [11] used the unified strength theory to combine the Weibull distribution to get the microunit strength; also, the modified model determines the height. Xing et al. [12] proposed a completely model thermoplastic constitutive for Tournemire shale which includes the hydrostatic-pressure-dependent and stress deviator-dependent initial/critical yield parameters that are quadratically at the same time linearly related to temperatures. Wang et al. [13] demonstrate that nanoemulsion liquid is more advantageous than distilled water for enhancing fracture complexity. Schuster et al. [14] studied that the weak clay-rich layer has a strong influence on the deformation behaviour.

At present, the research methods for the rock damage constitutive model mainly include two types: one is to obtain the stress and strain equations of the rock mass based on the test results and verified by a large number of test data [15–17]. The advantage of this method is that it is highly targeted. The other method is assuming that the microelement strength of the rock follows a certain distribution and the stress and strain equations of the rock are established through a certain derivation as well as compared with the test results [5, 6]. The advantage is that it has a wide range of applications, so it has become the main method for studying damage constitutive models. The statistical damage constitutive model can directly and accurately describe the defects of the rock damage evolution process to better describe the mechanical mechanism of rock damage [18–22].

The temperature has thermal damage to the rock which has been confirmed by a large number of research results [23–29]. Graves et al. [30] studied the temperature influence on rock strength and mechanical properties through high-power lasers. The microcracks vaporize cementation and dehydrate clay due to the high temperature as well as promote the permeability and porosity and decrease strength. Masri et al. [31] presented the thermal effect on anisotropic Tournemire shale which illustrates the elastic behaviour of shale is nonlinear. The confining pressure, temperature, and loading direction determined the failure mode in which the tensile failure and sliding failure are the main failure mechanisms. Xu et al. [32] conducted the tests on the state of rock deformation and destruction during the thermal stimulation of the heavy oil sand reservoirs. Masri et al. [33] studied Tournemire shale mechanical behaviour under the temperature and failure behaviours strongly affected by temperature variation. Zhu et al. [34] studied the physical and mechanical properties of sandstone with cracks after high temperature. It investigates that the volume of sandstone expands and the density decreases with increasing temperature. The failure mode is not only greatly affected by temperature but also related to the inclination of internal cracks. Zhu et al. [35] reviewed the mechanical properties of Chinese marble under high temperature and after temperature. The high-temperature effect on marble mechanical properties is in the primary microcracks and the development of new microcracks. Suo et al. [29] investigated the Lujiaping formation shale uniaxial compression strength and wave velocity measurements were performed. It concluded heating can change the water saturation and organic matter content of shale as well as shale has a strong anisotropy [36]. So far, few researchers consider the effect of shale under thermal and confining pressure conditions [37]. Therefore, the failure behaviours of shale in a deep environment are still unclear. Yan et al. [38] studied thermo-hydromechanical coupling crack propagation pattern based on the triaxial SC-CO$_2$ fracturing test system. The injection pressure evolution was analyzed, and the fracture number, length, and propagation directions of the sample surface were determined [39].

In this paper, a preliminary statistical constitutive model for thermal damage of shale under triaxial compression is proposed which takes into account the thermal damage effect of temperature. The different shale physical parameters are tested under different target temperatures (25, 200, 400, and 600°C), through the triaxial compression test of
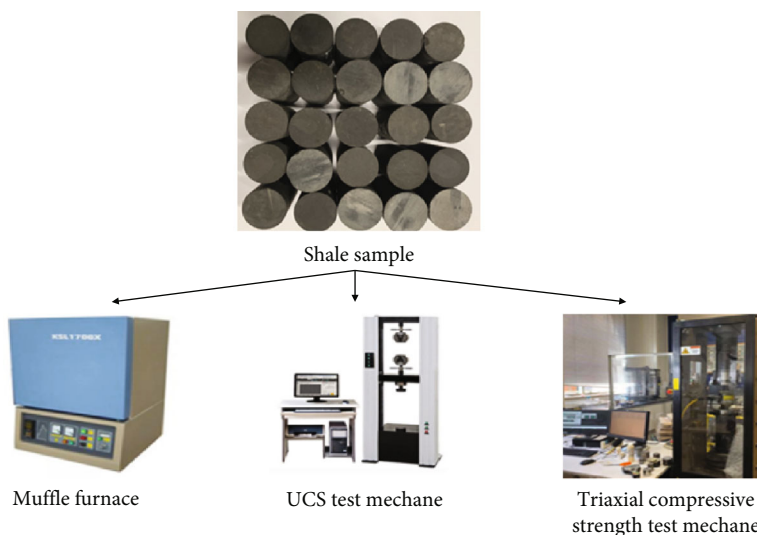
shale specimens after high temperature to verify the proposed constitutive model.

2. Test Equipment and Procedure

Figure 1 shows the whole experimental apparatus and process in this work. The test shale samples were taken from the Longmaxi Formation, Chongqing, Southwest of China. The density of the shale sample is $2600 \, \text{kg/m}^3$. The size of the sample is standard which is 25 mm in diameter and 50 mm in length. The unevenness of both ends of the test piece is not more than 0.02 mm, and the error in the height of the test piece is no more than 0.1 mm. The shale samples were put into a box-type resistance furnace to heat to a certain temperature. The equipment uses silicon carbon rod element heating and high-performance fiber insulation which can realize automatic heating and temperature control. The maximum design temperature is 600°C. In the test, the temperature is set as 25, 200, 400, and 600°C, there are a total of 4 temperature grades, and each group has 9 samples. After heating to a preset temperature at a rate of 1°C/min, the temperature is kept constant for 24 h. After that, it naturally cooled to room temperature in the furnace and finally, shale samples with different heating temperatures are obtained. The main mineral component of shale is quartz (45%), clay minerals (16%), calcite (22%), dolomite (11%), etc. All shale samples are measured for quality and size before heating and after heating. The triaxial compression test is carried out on the MTS-810 electrohydraulic servo control test system which measures the axial compression deformation with a 5 mm displacement sensor and 1000 kN force sensor to measure axial load. The test adopts the displacement control mode as well as the loading rate set as 0.005 mm/s. During the test, the load and deformation are automatically collected and displayed in real time. The test system can obtain the whole stress-strain curve of the specimen during triaxial compression.

3. Experimental Results

3.1. The Unconfined Compressive Strength of Shale. The shale unconfined compressive strength is the load per unit area of the shale specimen from uniaxial compression to failure. There are 12 samples to test UCS, and each target temperature (25, 200, 400, and 600°C) has three samples. Figure 2 illustrates the unconfined compressive strength of shale values at different temperatures. In the experiment, to prevent shale sample failure during the experiment, the rubber is used to stick the shale sample. The typical stress-strain curve is divided into four stages: the compaction stage, elastic stage, yield stage, and failure stage. In the compaction stage, the stress-strain curve is upward concave. As stress increases, the deformation develops faster. This is mainly due to the closure of microcracks in the rock under the action of external force. In the approximate linear elastic deformation stage, the curve at this stage is approximately straight. The stress and strain are proportional as well as the slope of the curve in this straight line is the elastic modulus. In the failure stage, the sample reached the uniaxial compression strength value and failure occurred. The stress-strain curves of shale samples are quite different after keeping them at different temperatures. As the temperature rises, the stress curve peak point gradually moves down and the strain also decreased. As the temperature rises, the curve peak stress point gradually moves down, and the strain also decreased. This may be after high-temperature action, microcracks increased and thermal damage occurred inside the shale sample. As a result, the mechanical strength of shale samples decreases and is easy to damage.

3.2. The Triaxial Compressive Strength of Shale. The triaxial compressive experiment is an effective method to test the shale sample under in situ conditions. The triaxial compressive strength value of the shale sample is influenced by temperature. When the shale is affected by temperature, the various mineral crystals that make up the rock have different

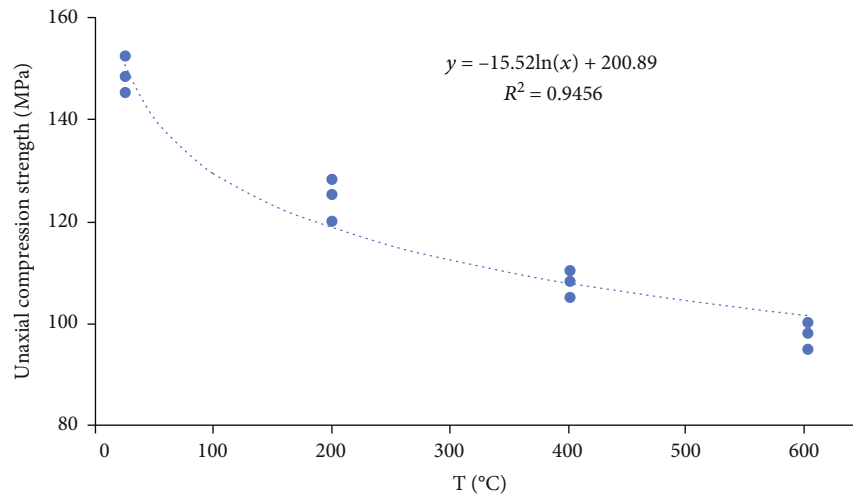$$y = -15.52\ln(x) + 200.89$$
$$R^2 = 0.9456$$

FIGURE 2: The UCS value change with the temperature.

thermal expansion coefficients. The various mineral particles inside cannot be freely deformed with temperature according to their own inherent thermal expansion coefficients in order to maintain the continuity of rock deformation. It leads to constraints between minerals and particles. The large deformation is compressed, and the small deformation is stretched. This is the so-called thermal stress. When the temperature is higher, there will inevitably be a large number of microcracks in the rock and it will gradually expand as the temperature rises resulting in a significant reduction in the elastic modulus. It is convinced that the temperature has caused damage to the rock [25, 40]. It can be seen in Figure 3 that with the confining pressure increase, the triaxial compressive strength value gradually increases as well as the shale triaxial compressive strength has a negative effect on the temperature.

3.3. The Failure Mode of Shale. The failure mode of shale is related to many factors such as loading conditions, temperature, lithology, and internal structure [13, 41, 42]. The test confining pressure condition is the main factor affecting the failure mode of shale as well as the different mineral compositions caused by temperature also drive the failure mode of shale. In our experiment results, there are two main failure modes of black shale in the test: splitting failure and shear failure. The failure modes of shale samples under different confining pressures and temperatures are shown in Table 1. When the confining pressure is zero, the shale generates a multilayered bedding plane splitting failure. The reason is that the original defects such as pores and fractures are mostly distributed to the bedding plane and then original defects develop, expand, and connect formed fracture. It can be seen that the number of fractures at high temperatures is lower than at low temperatures. In the confining pressure 15 MPa condition, the bedding and lamellar minerals of shale samples are compacted. The splitting failure mode decreases gradually under the high confining pressure. Under the confining pressure, the shale mineral particles produce shear cracks due to stress concentration; furthermore, it is further developed into a shear plane

through multiple bedding planes. Under the confining pressure 30 MPa, the compaction degree between bedding and flaky minerals is higher with the increase of confining pressure. They are reconstituted with other minerals to form structural bodies, and failure occurs. Compared with low confining pressure, there is no complex fracture network and the failure surface of the shale sample is a single shear plane.

3.4. Consider the Effect of Temperature on Elastic Modulus and Poisson's Ratio. From the following Figure 4, we can analyze the change of shale elastic modulus with temperature after high temperature under different confining pressures. When the confining pressure is constant, the elastic modulus of shale decreases with the increase of real-time temperature due to the temperature effect. The internal components of the shale rock sample began to expand unevenly which led to the rapid generation of a large number of microscopic defects, thereby reducing the stiffness of the shale and greatly weakening the ability to resist deformation. This is the main reason that leads to a rapid decrease in the modulus of elasticity. Under different confining pressures, the change law of elastic modulus with increasing temperature is unchanged; however, the overall elastic modulus of shale is higher than that under low confining pressure. The reason is that confining pressure increase closes the thermal damage cracks to a certain extent, compacts the pores in the shale, and slightly improves the ability of the shale to resist deformation.

$$E^* = -0.0638T + 51.415(15\,\mathrm{MPa}), \tag{1}$$

$$E^* = -0.0648T + 55.96(30\,\mathrm{MPa}). \tag{2}$$

As it can be shown from Figure 5 that under the condition of a certain confining pressure, the Poisson ratio of the shale sample gradually increases with the increase of temperature. This is because as the temperature increases, the internal structure of the shale sample changes, which promotes the increase in Poisson's ratio to a certain extent. Under
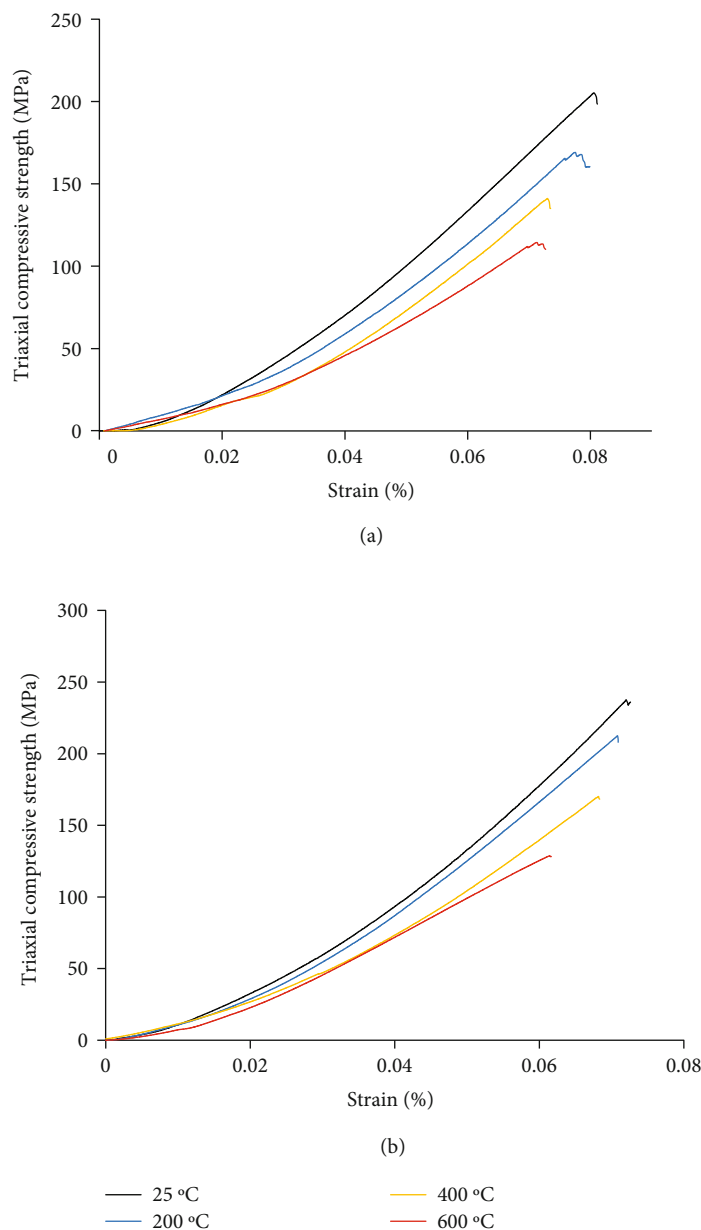
FIGURE 3: The triaxial compressive strength range with the temperature. (a) The triaxial compressive strength under confining pressure 15 MPa; (b) The triaxial compressive strength under confining pressure 30 MPa.

different confining pressures, the Poisson ratio of the shale sample increased slightly and was higher than that of the shale sample under low confining pressure. The microcracks in the shale remain closed, and the internal voids are gradually compacted, resulting in the overall Poisson ratio of the shale sample being higher than the Poisson ratio under low confining pressure.

4. Statistical Damage Constitutive Model for Shale

4.1. Constitutive Model without considering Temperature Thermal Damage. There are a large number of pores, cracks, and other defects inside the rock, and they are randomly distributed. The mechanical properties of the constituent com-

ponents of the rock cannot be expressed by a single parameter equation. In this section, the damage evolution equation is established and the analysis method of probability statistics is introduced in this section, combined with damage mechanics to study the constitutive relationship of rock which has very important theoretical significance.

Assume that the strength of the rock microelement obeys the Weibull distribution and the statistical distribution law of the rock microelement strength is calculated based on the Weibull distribution. The formula as follows (1):

$$P(x) = \frac{M}{F_0} \left(\frac{x}{F_0} \right)^{M-1} \exp \left[-\left(\frac{x}{F_0} \right)^M \right]. \tag{3}$$

TABLE 1: The failure mode of shale under different temperatures and confining pressures.

Temperature	Failure mode		
25°C			
	0 MPa	15 MPa	30 MPa
200°C			
	0 MPa	15 MPa	30 MPa
400°C			
	0 MPa	15 MPa	30 MPa
600°C			
	0 MPa	15 MPa	30 MPa

x is the microstrain of the rock. M and F_0 are the distribution scale of the Weibull distribution and the morphological parameter characterized by strain. $P(x)$ is the probability of failure of microcomponents under strain.

Based on the assumption that the strength of the elastic part obeys the statistical distribution, the elastic part will gradually fail to reflect this gradual process when the load gradually increases. The concept of damage mechanics is led into the equation. It is assumed that the rock failure is caused by these continuous microelements. The number of damaged microelements under a certain level of load is N_d; then, the statistical damage variable is the ratio of the damaged elastic body to the total number of microelements N, so the expression of the damage variable under a certain level of load is (2)

$$D = \frac{N_d}{N}. \qquad (4)$$

D is the statistical damage variable, N_d is number of microelements that have expired, and N is total number of microelements.

Similarly, it is also assumed that the failure probability of cumulative stress of microelement elastic is as follows ((3), (4)):

$$\rho f = \rho(F)dF, \qquad (5)$$

$$dN_d = N\rho f = N\rho(F)dF. \qquad (6)$$

ρ is the density function, dN_d is the number of failed microelements, and N is the total number of microelements.

Under the effect of loading pressure, the internal fractures of the rock begin initiation, propagation, and slit linked up. The damage parameter D is a description of the cumulative effect of the microelement failure during the loading process of the rock. It is believed that the microelements with strength less than the stress level F have also failed when it is loaded to a certain stress level. The number of failed microelements in the rock block dN is the sum of the number of failed microelements in the previous intervals, such as formula (5).

$$N_D = \int_{-\infty}^{F} N\rho(F)dF = N\rho(F). \qquad (7)$$

It is also assumed that the failure criterion of the rock is equation (6):

$$f(\sigma^*) - k_0 = F - k_0 = 0. \qquad (8)$$

F is the microelement stress level and k_0 is the material strength.

In the 1970s, Lemaitre put forward the hypothesis of strain equivalence, and then, the basic relationship of rock damage constitutive equation is established as follows ((7)):

$$\sigma = \sigma^*(1 - D) = E\varepsilon(1 - D). \qquad (9)$$

σ is the nominal stress tensor, σ^* is the effective stress tensor, D is the load damage variable, E is the material elasticity tensor, and ε is the strain tensor.

Then, take (7) into (5) to calculate that the distribution function of the two-parameter Weibull distribution of rock microelement is

$$P(x) = 1 - \exp\left[-\left(\frac{x}{F_0}\right)^M\right]. \qquad (10)$$

M and F_0 are statistical parameters; then, from (8),

$$D = P(F) = 1 - \exp\left[-\left(\frac{F}{F_0}\right)^M\right]. \qquad (11)$$

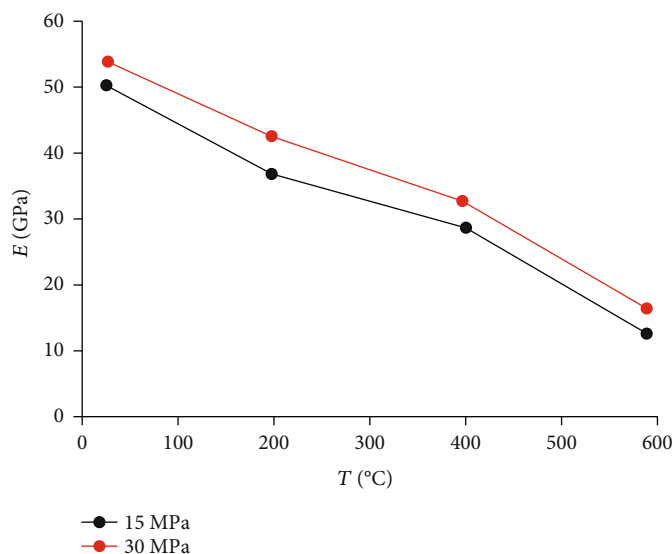Equation (9) is the derived statistical damage evolution equation.

FIGURE 4: Changes of shale elastic modulus with temperature after high temperature under different confining pressures.
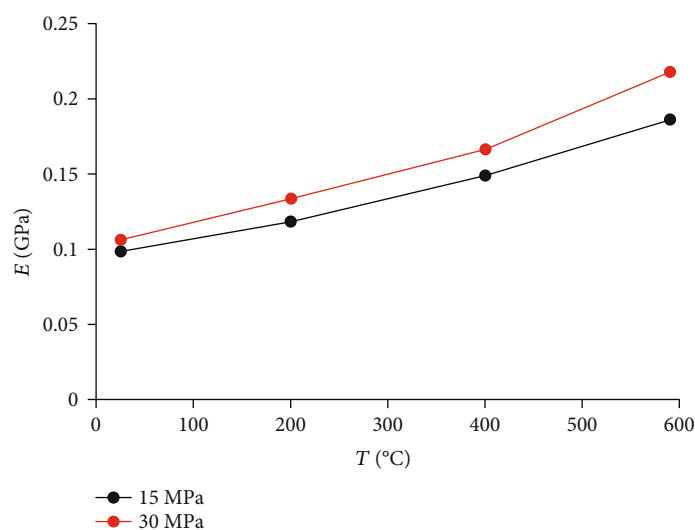

FIGURE 5: Changes of shale elastic modulus with temperature after high temperature under different confining pressures.

Among of them, M and F_0 are the statistical parameter.

The different M of Weibull distribution density function and distribution function are shown in Figures 6 and 7. Like the lognormal distribution, the domain of the Weibull distribution is also a positive real number. Therefore, Weibull is also very suitable for the study of the statistical damage constitutive relationship of rock. When the dispersion of the Weibull distribution decreases, the random variable tends to shift in the left and right directions. Compared to the lognormal distribution, the Weibull distribution is a less conservative type of distribution. It reflects the distribution of random variables to a certain extent.

4.2. Establish a Statistical Damage Constitutive Model of Rock. From equation (9), the parameter F is unknown, so

the f function in equation (6) needs to be reified. In this paper, the commonly used yield criterion expression of rock materials is used.

Based on the D-P failure criterion, this paper establishes the expression method of rock microelement strength. The rock element strength F based on the D-P failure criterion can be expressed as

$$f(\sigma) = \alpha_0 M_1 + \sqrt{M_2}. \tag{12}$$

$\alpha_0 = \sin \varphi / \sqrt{9 + 3 \sin^2\varphi}$, φ is the internal friction angle of rock, M_1 is the first invariant, and M_2 is the second invariant.
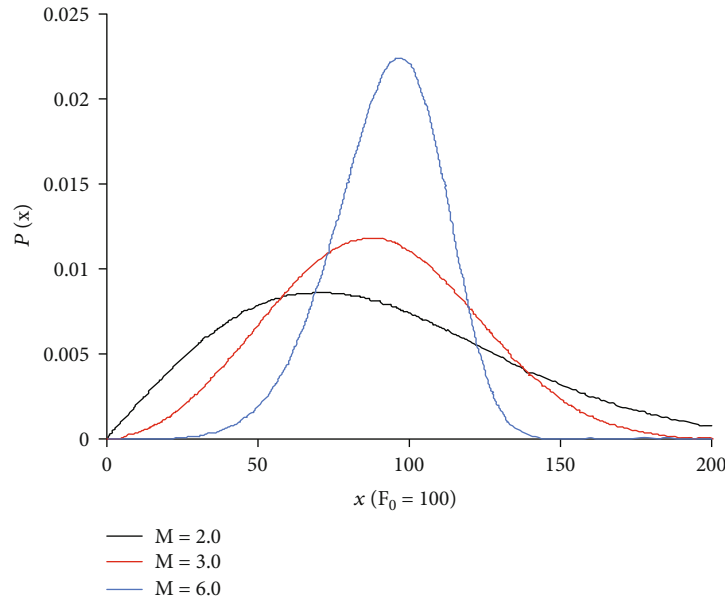
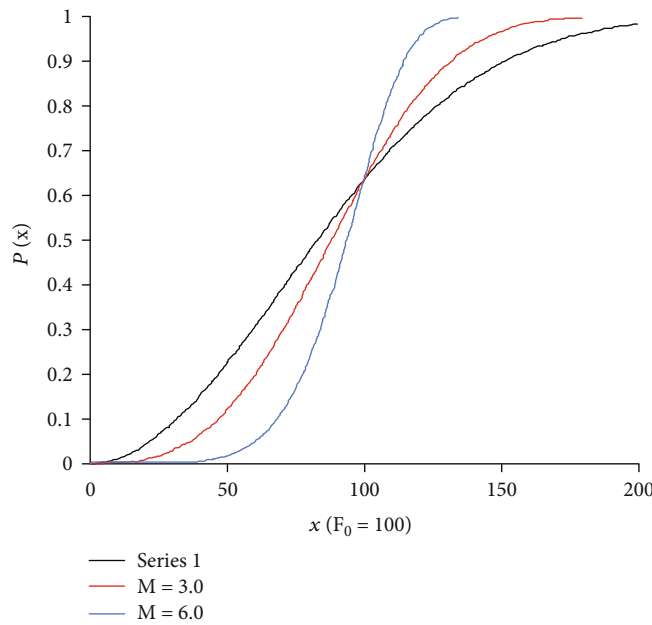FIGURE 6: The density function of the Weibull distribution.

FIGURE 7: Distribution function of Weibull distribution.

By the strain tensor calculation formula,

$$M_1 = \sigma_1^* + \sigma_2^* + \sigma_3^*, \tag{13}$$

$$M_2 = \frac{1}{6}\left[(\sigma_1^* - \sigma_2^*)^2 + (\sigma_2^* - \sigma_3^*)^2 + (\sigma_3^* - \sigma_1^*)^2\right]. \tag{14}$$

Obtain the nominal stress $\sigma_1, \sigma_2, \sigma_3$ ($\sigma_2 = \sigma_3$, pseudo-triaxial) and strain from the triaxial test$\varepsilon_1, \varepsilon_2, \varepsilon_3$, and the

corresponding effective stress is $\sigma_1^*, \sigma_2^*, \sigma_3^*$ ($\sigma_2^* = \sigma_3^*$). The damage variable is introduced, and the effective stress can be calculated by formula (13):

$$\sigma_1^* = \frac{\sigma_1}{1 - \delta D}, \tag{15}$$

$$\sigma_2^* = \sigma_3^* = \frac{\sigma_3}{1 - \delta D}. \tag{16}$$

Assuming that the rock failure conforms to the Mises yield criterion, the strain expression can be obtained from the general Hooke law:

$$\varepsilon_1 = \frac{(\sigma_1^* - 2\mu\sigma_3^*)}{E^*}. \tag{17}$$

Bring (13) and (15) into (11) to get
E^* is changed in the different conditions.

$$M_1 = \frac{(\sigma_1 + 2\sigma_3)E^*\varepsilon_1}{\sigma_1 - 2\mu\sigma_3}, \tag{18}$$

$$\sqrt{M_2} = \frac{(\sigma_1 - \sigma_3)E^*\varepsilon_1}{\sqrt{3}(\sigma_1 - 2\mu\sigma_3)}. \tag{19}$$

ε_1 is the main strain, μ is Poisson's ratio, and E is elastic modulus.

The microelement strength of the rock can be expressed as

$$f(\sigma) = \frac{E^*\varepsilon_1}{\sigma_1 - 2\mu\sigma_3}\left[\left(\alpha_0 + \frac{\sqrt{3}}{3}\right)\sigma_1 + \sigma_3\left(2\alpha_0 - \frac{\sqrt{3}}{3}\right)\right]. \tag{20}$$

By substituting (17) and (9) into equation (14), the constitutive equation of rock damage is derived as follows:

$$\sigma_1 = E^*\varepsilon_1(1 - D) + \mu(\sigma_1 + \sigma_2) = E^*\varepsilon_1 \exp\left[-\left(\frac{F}{F_0}\right)^M\right] + 2\mu\sigma_3,$$

$$\sigma_3 = \frac{E^*\varepsilon_3 \exp\left[-(F/F_0)^M\right]}{1 - \mu} + \frac{\mu\sigma_1}{1 - \mu}. \tag{21}$$

It can be observed from the derivation (19) that the determination of M and F_0 model parameters directly affects the establishment of the rock damage constitutive equation.

4.3. *Statistical Parameters of Damage Constitutive Model.* There are two main methods for determining model parameters: (1) linear fitting method and (2) peak point method. The characteristic of the linear fitting method is to fully consider the full stress-strain curve of rock compression, that is, to consider the same weight for any point on the test curve. For specific rock triaxial compression test data, the statistical parameters can be determined by the linear fitting method. Since the true stress-strain curve cannot be obtained directly from the triaxial compression test, when the specific parameters are determined, the statistical damage constitutive equation expressed by the measured stress and strain can be used to match the measured stress-strain curve. Therefore, this paper adopts linear simulation. It is legal to determine the model parameters.

Based on the uniaxial compression experiment of rock, let $\sigma_2 = 0, \sigma_3 = 0$, bring it into the above formula

(19), and take the logarithm of both sides at the same time to obtain

$$-\ln\left(\frac{\sigma_1}{E^*\varepsilon_1}\right) = \left(\frac{F}{F_0}\right)^m, \tag{22}$$

where $\alpha = (1/F_0)^m$ brings in and simplifies

$$-\ln\left(\frac{\sigma_1}{E^*\varepsilon_1}\right) = \alpha F^m. \tag{23}$$

Take the logarithm of both sides at the same time to get

$$\ln\left[-\ln\left(\frac{\sigma_1}{E^*\varepsilon_1}\right)\right] = \ln \alpha + m \ln F. \tag{24}$$

Let $Y = \ln\left[-\ln\left(\sigma_1/E^*\varepsilon_1\right)\right]$, $X = \ln F$, and $b = \ln \alpha$ bring into simplification:

$$Y = aX + b. \tag{25}$$

From this linear fitting, the m and b values can be obtained, so that

$$F_0 = \exp\left(-\frac{b}{m}\right). \tag{26}$$

4.4. *The Damage Constitutive Model of Shale under Thermal-Mechanical Coupling.* Under the action of real-time temperature, the thermal expansion between different minerals in the shale produces squeezing stress and violent thermal movement between the molecules which causes thermal stress in the shale. A large number of thermal damage defects are generated from microcosmic and then reflect the macroscopic phenomena. Due to the accumulation of microdefects, the macrocracks finally show the gradual propagation and penetration. The process of macroscopic damage to shale caused by microscopic accumulation is expressed by thermal damage variables D_T.

According to the theory of macroscopic damage mechanics, rock microcracks continue to grow under thermal-mechanical coupling and thermal-mechanical coupling damage occurs to shale. So the thermal-mechanical coupling damage variable is defined.

$$D_T = 1 - \frac{E_T}{E_0}. \tag{27}$$

E_T the elastic modulus of the rock at different real-time temperatures; E_0 is the elastic modulus of rock at room temperature.

The total damage formula deduced in the literature [43]:

$$D_m = D + D_T - DD_T. \tag{28}$$
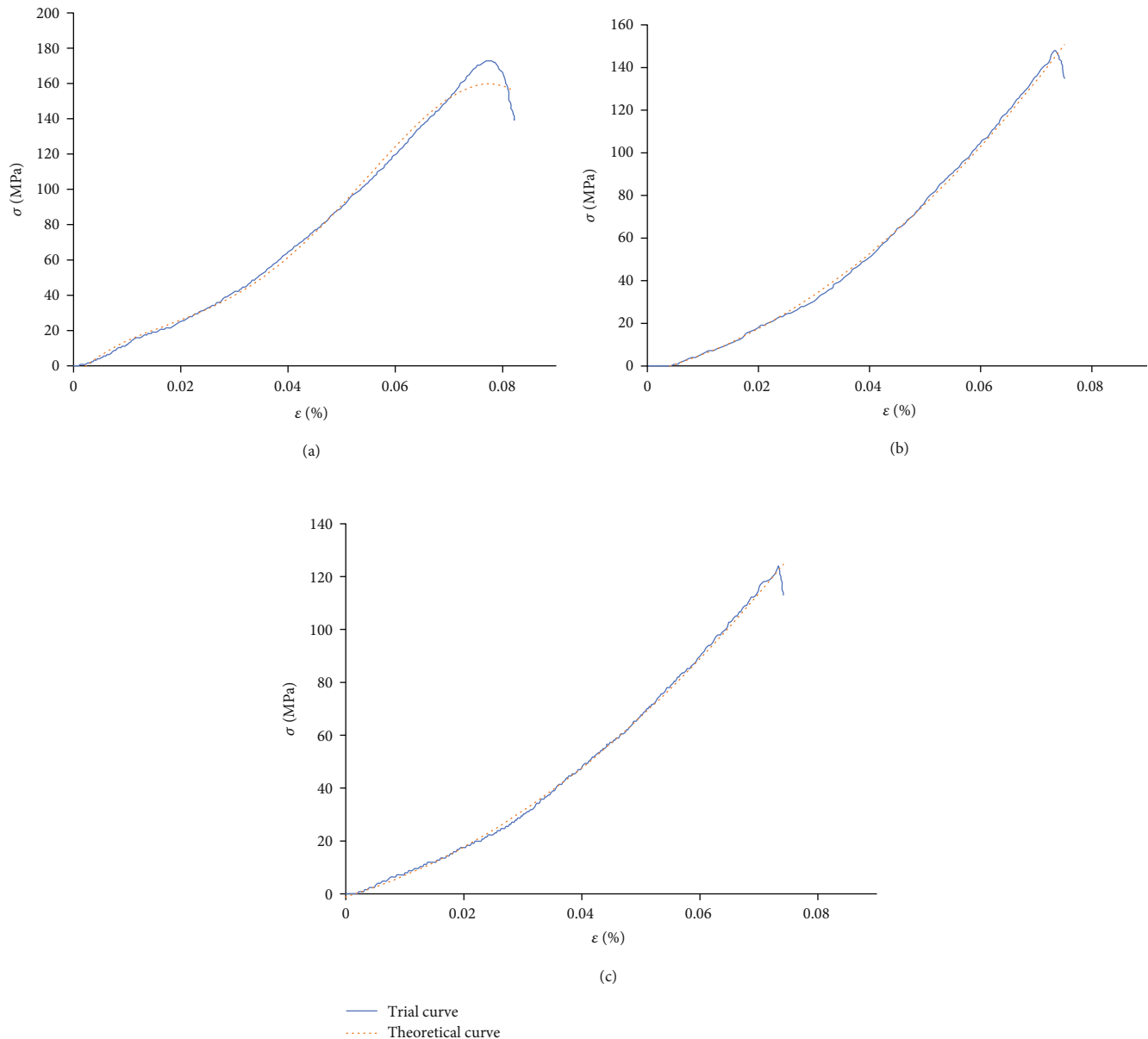
(a)

(b)

(c)

Trial curve
Theoretical curve

FIGURE 8: Comparison of theoretical curve and experimental curve under 15 MPa confining pressure. (a) Temperature 200°C, confining pressure 15 MPa; (b) Temperature 400°C, confining pressure 15 MPa; (c) Temperature 600°C, confining pressure 15 MPa.

Then, (9) and (25) are brought into (26) to obtain the total damage evolution of shale under the coupled thermal-mechanical action. The equation is as follows:

$$D_m = 1 - \frac{E_T}{E_0} \exp\left[-\frac{1}{M}\left(\frac{F}{F_0}\right)^M\right]. \tag{29}$$

5. Model Verification

In order to verify the damage statistical model established in this paper and to determine the model parameters, this paper selects shale as the sample and starts the triaxial compression experiment. Through the expansion of triaxial compression experiments under different confining pressures and different temperatures, the comparison between the experimental curve and the theoretical calculation curve is obtained as shown in Figures 8 and 9. The results show that although the theoretical calculation curve and the value obtained from the experimental curve are not completely consistent, the trend is basically the same and the error is also high. In a small range, it can meet the needs of actual engineering calculations, especially the theoretical curve before the peak point, which shows different initial points of damage under different confining pressures, including both the linear elastic deformation stage
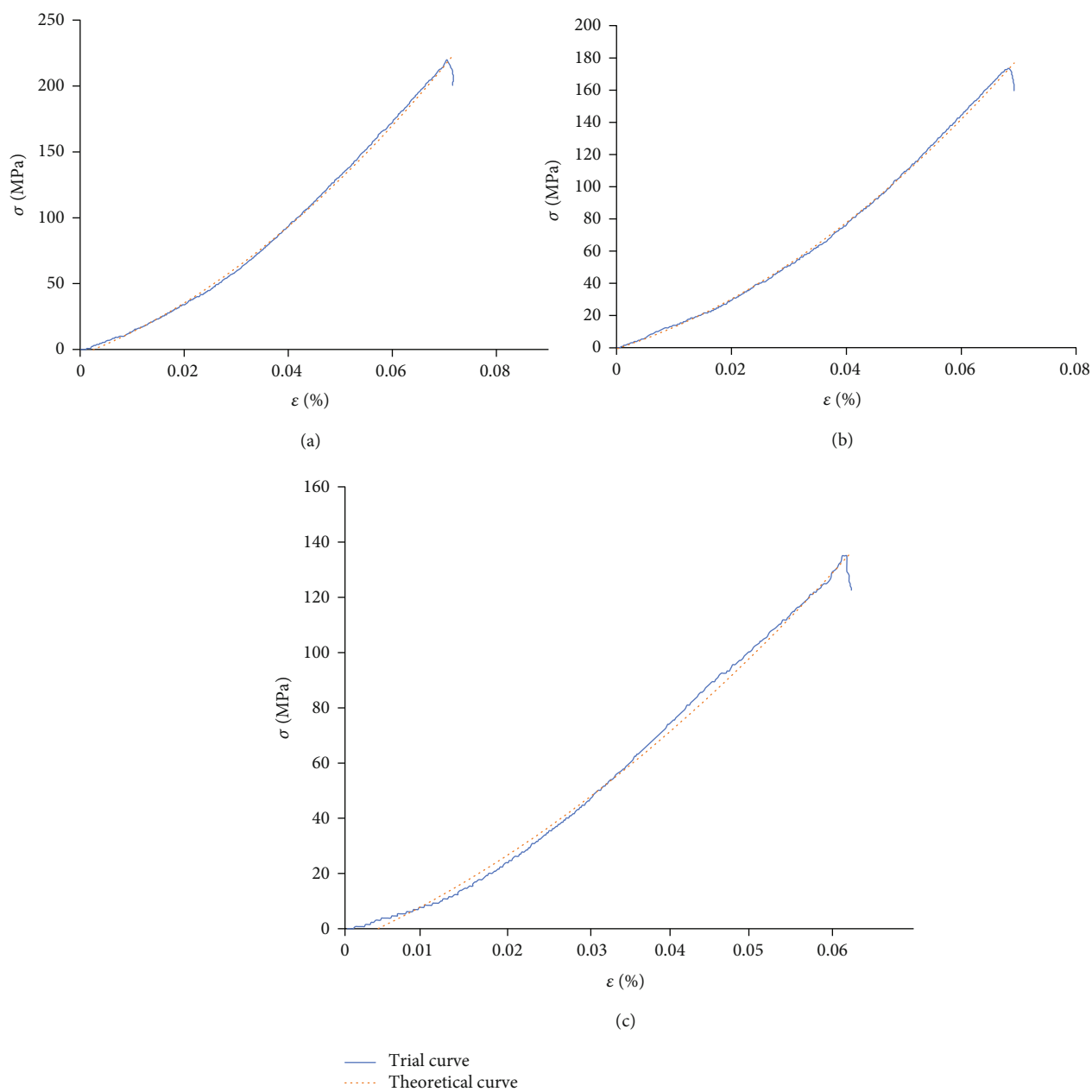
Figure 9: Comparison of theoretical curve and experimental curve under 30 MPa confining pressure. (a) Temperature 200°C, confining pressure 30 MPa; (b) Temperature 400°C, confining pressure 30 MPa; (c) Temperature 600°C, confining pressure 30 MPa.

and the postdamage. In the elastoplastic stage, the effect of matching the actual curve is very good, and it is more in line with the actual situation.

The rock statistical damage constitutive model established based on the Weibull distribution theory can better reflect the stress-strain characteristics in the process of rock deformation and failure. Under the condition of a certain confining pressure, the compressive strength of shale gradually increases with the increase of temperature. Decrease indicates that the mechanical properties of shale deteriorate after high temperature; high temperature has damage to the rock; the peak strain of rock increases with the increase of temperature; the stress-strain curve moves to the right with the increase of temperature, indicating that with the increase of temperature, the plastic deformation of large rocks increases, and at the same time, the theoretical curve of shale stress-strain fits better with the experimental curve. When the temperature is the same, as the confining pressure increases, the compressive strength of the shale gradually increases, indicating that the confining pressure has the effect of increasing the strength of the rock, and the greater the confining pressure, the higher the degree of agreement between the curves. It is worth noting that the failure process of rock under peusdostatic load is very complicated.

Although the constitutive model established in this paper has certain advantages, it cannot essentially explain the failure mechanism of rock. Therefore, related theories need to be further explored.

6. Conclusions

In this paper, a series of mechanical and physical parameters of shale are tested. Firstly, basic physical properties of shale are analyzed. After that, the stress-strain curve and failure mode of shale under high temperature and pressure are analyzed. Finally, the damage constitutive equation of shale is established.

(1) When the temperature is constant, the elastic modulus of shale increases with the increase of confining pressure. With the increase of temperature, the peak strength of shale is low. The confining pressure can effectively improve the strength of shale

(2) The stress-strain curve of shale has obvious pore and fracture in the compaction stage. In the linear stage, the stress-strain curve before the peak is approximately a straight line. Under the condition of low confining pressure, it is easy to form more complex fracture network. Under high confining pressure, the fracture formed a single fracture. From the low confining pressure to high confining pressure, it shows strong plastic deformation and failure characteristics

(3) The real-time triaxial compression test data of shale under high temperature and high pressure are used to calculate and compare the model. The established model can well predict the mechanical properties of shale under high temperature and high pressure

Data Availability

The data used to support the findings of this study are all shown in the uploaded manuscript.

Conflicts of Interest

The authors declare that they have no conflicts of interest.

Acknowledgments

References

[1] Y. H. Wang, B. H. Ju, S. H. Wang, Z. Z. Yang, and Q. Liu, "A tight sandstone multi-physical hydraulic fractures simulator study and its field application," *Petroleum*, vol. 6, no. 2, pp. 198–205, 2020.

[2] L. M. Kachanov, "Time of the rupture process under creep conditions, Izy Akad," *Nank SSR Otd Tech Nauk*, vol. 8, pp. 26–31, 1958.

[3] J. W. Dougill, "Mechanics in engineering," *ASCE EMD*, pp. 333–355, 1976.

[4] L. Gambarotta and S. Lagomarsino, "A microcrack damage model for brittle materials," *International Journal of Solids Structures*, vol. 30, no. 2, pp. 177–198, 1993.

[5] S. W. Yu and X. Q. Feng, "A micromechanics-based damage model for microcrack-weakened brittle solids," *Mechanics of Materials*, vol. 20, no. 1, pp. 59–76, 1995.

[6] J. Zhou, W. Y. Xu, and X. G. Yang, "A microcrack damage model for brittle rocks under uniaxial compression," *Mechanics Research Communications*, vol. 37, no. 4, pp. 399–405, 2010.

[7] E. Hamdi, N. B. Romdhane, and L. Clech, "A tensile damage model for rocks: application to blast induced damage assessment," *Computers and Geotechnics*, vol. 38, no. 2, pp. 133–141, 2011.

[8] G. Li and C. A. Tang, "A statistical meso-damage mechanical method for modeling trans-scale progressive failure process of rock," *International Journal of Rock Mechanics Mining Sciences*, vol. 74, pp. 133–150, 2015.

[9] S. Huang, Q. Liu, A. Cheng, and Y. Liu, "A statistical damage constitutive model under freeze-thaw and loading for rock and its engineering application," *Cold Regions Science Technology*, vol. 145, pp. 142–150, 2018.

[10] K. Bian, J. Liu, W. Zhang, X. Zheng, S. Ni, and Z. Liu, "Mechanical Behavior and Damage Constitutive Model of Rock Subjected to Water-Weakening Effect and Uniaxial Loading," *Rock Mechanics Rock Engineering*, vol. 52, no. 1, pp. 97–106, 2019.

[11] P. Shen, H. Tang, D. Wang, Y. Ning, Y. Zhang, and X. Su, "A statistical damage constitutive model based on unified strength theory for embankment rocks," *Marine Georesources Geotechnology*, vol. 38, no. 7, pp. 818–829, 2019.

[12] Y. Xing, G. Zhang, and S. Li, "Thermoplastic constitutive modeling of shale based on temperature-dependent Drucker-Prager plasticity," *International Journal of Rock Mechanics Mining Sciences*, vol. 130, article 104305, 2020.

[13] Y. Wang and C. H. Li, "Investigation of the P-and S-wave velocity anisotropy of a Longmaxi formation shale by real-time ultrasonic and mechanical experiments under uniaxial deformation," *Journal of Petroleum Science Engineering*, vol. 158, pp. 253–267, 2017.

[14] V. Schuster, E. Rybacki, A. Bonnelye, J. Herrmann, A. M. Schleicher, and G. Dresen, "Experimental deformation of Opalinus Clay at elevated temperature and pressure conditions mechanical properties and the influence of rock fabric," *Rock Mechanics and Rock Engineering*, vol. 54, no. 8, pp. 4009–4039, 2021.

[15] C. A. Tang and X. H. Xu, "Statistical damage analysis of the rock complete stress–strain process," *Journal of Northeast University of Technology*, vol. 51, no. 2, pp. 191–195, 1987.

[16] H. Zhang, Z. Wan, C. Wang, Z. Ma, Y. Zhang, and J. Cheng, "A statistical damage constitutive model for geomaterials under plane-strain biaxial stress state," *Advances in Mathematical Physics*, vol. 2017, Article ID 3807401, 10 pages, 2017.

[17] T. Bruning, M. Karakus, G. D. Nguyen, and D. Goodchild, "An experimental and theoretical stress-strain-damage correlation procedure for constitutive modelling of granite," *International Journal of Rock Mechanics Mining Sciences*, vol. 116, pp. 1–12, 2019.

[18] C. Wen, F. Zu, and J. Xue, "A study of statistical constitutive model for soft and damage rocks," *Chinese Journal of Rock Mechanics*, vol. 17, no. 6, pp. 628–633, 1998.

[19] W. G. Cao, X. Li, and H. Zhao, "Damage constitutive model for strain-softening rock based on normal distribution and its parameter determination," *Journal of Central South University of Technology*, vol. 14, no. 5, pp. 719–724, 2007.

[20] X. Li, W. G. Cao, and Y. H. Su, "A statistical damage constitutive model for softening behavior of rocks," *Engineering Geology*, vol. 143, pp. 1–17, 2012.

[21] Y. Wang and C. H. Li, "Investigation of the P- and S-wave velocity anisotropy of a Longmaxi formation shale by real-time ultrasonic and mechanical experiments under uniaxial deformation," *Journal of Petroleum Science Engineering*, vol. 158, pp. 253–267, 2017.

[22] X. F. Guo, N. Nan, B. X. Liu et al., "An improved creep damage mechanics model and its application to evaluate creep strain design codes for hot outlet manifold in steam reformer furnace," *International Journal of Pressure Vessels and Piping*, vol. 198, article 104649, 2022.

[23] W. Somerton, M. Mehta, and G. W. Dean, "Thermal alteration of sandstones," *Journal of Petroleum Technology*, vol. 17, no. 5, pp. 589–593, 1965.

[24] D. Richter and G. Simmons, "Thermal expansion behavior of igneous rocks," *International Journal of Rock Mechanics and Mining Sciences & Geomechanics Abstracts*, vol. 11, no. 10, pp. 403–411, 1974.

[25] C. Yong and C. Wang, "Thermally induced acoustic emission in Westerly granite," *Geophysical Research Letters*, vol. 7, no. 12, pp. 1089–1092, 1980.

[26] M. Hettema, K. A. Wolf, and D. Pater, "The influence of steam pressure on thermal spalling of sedimentary rock: theory and experiments," *International Journal of Rock Mechanics Mining Sciences*, vol. 35, no. 1, pp. 3–15, 1998.

[27] S. Djaknoun, E. Ouedraogo, and A. Ahmed Benyahia, "Characterisation of the behaviour of high performance mortar subjected to high temperatures," *Construction Building Materials*, vol. 28, no. 1, pp. 176–186, 2012.

[28] H. Kim, J. W. Cho, I. Song, and K. B. Min, "Anisotropy of elastic moduli, P-wave velocities, and thermal conductivities of Asan Gneiss, Boryeong Shale, and Yeoncheon Schist in Korea," *Engineering Geology*, vol. 147, pp. 68–77, 2012.

[29] Y. Suo, Z. Chen, and S. S. Rahman, "Changes in shale rock properties and wave velocity anisotropy induced by increasing temperature," *Natural Resources Research*, vol. 29, no. 6, pp. 4073–4083, 2020.

[30] R. M. Graves, S. Batarseh, R. A. Parher, and B. C. Gahan, "Temperatures induced by high power lasers: effects on reservoir rock strength and mechanical properties," in *SPE/ISRM Rock Mechanics Conference*, Irving, Texas, 2002Society of Petroleum Engineers.

[31] M. Masri, M. Sibai, and J. Shao, "Experimental study of the temperature effect on the mechanical behaviour of anisotropic rock," in *ISRM International Symposium on Rock Mechanics-SINOROCK 2009*, Hong Kong, China, 2009.

[32] B. Xu, Y. Yuan, and Z. Wang, "Thermal impact on shale deformation/failure behaviors—laboratory studies," in *45th US Rock Mechanics/Geomechanics Symposium*, San Francisco, California, 2011.

[33] M. Masri, M. Sibai, J. F. Shao, and M. Mainguy, "Experimental investigation of the effect of temperature on the mechanical behavior of Tournemire shale," *International Journal of Rock Mechanics Mining Sciences*, vol. 70, pp. 185–191, 2014.

[34] T. Zhu, H. Jing, H. Su, Q. Yin, M. Du, and G. Han, "Physical and mechanical properties of sandstone containing a single fissure after exposure to high temperatures," *International Journal of Mining Science Technology*, vol. 26, no. 2, pp. 319–325, 2016.

[35] Z. N. Zhu, H. Tian, G. S. Jiang, and W. Cheng, "Effects of high temperature on the mechanical properties of Chinese marble," *Rock Mechanics Rock Engineering*, vol. 51, no. 6, pp. 1937–1942, 2018.

[36] Y. Suo, Z. Chen, and S. Rahman, "Mixed-mode fracture behaviour of semicircular bend shale with bedding layer," *Arabian Journal for Science and Engineering*, vol. 46, no. 7, pp. 6967–6978, 2021.

[37] Y. Suo, Z. Chen, S. S. Rahman, and H. Song, "Experimental and numerical investigation of the effect of bedding layer orientation on fracture toughness of shale rocks," *Rock Mechanics and Rock Engineering*, vol. 53, no. 8, pp. 3625–3635, 2020.

[38] H. Yan, J. Zhang, B. Li, and C. Zhu, "Crack propagation patterns and factors controlling complex crack network formation in coal bodies during tri-axial supercritical carbon dioxide fracturing," *Fuel*, vol. 286, article 119381, 2021.

[39] Y. Suo, Z. Chen, S. S. Rahman, and X. Chen, "Experimental study on mechanical and anisotropic properties of shale and estimation of uniaxial compressive strength," in *Energy Sources, Part A: Recovery, Utilization, and Environmental Effects*, pp. 1–11, Taylor & Francis, 2020.

[40] A. Ferrero and P. Marini, "Experimental studies on the mechanical behaviour of two thermal cracked marbles," *Rock Mechanics and Rock Engineering*, vol. 34, pp. 57–66, 2001.

[41] X.-D. Wu, J.-R. Liu, and J.-S. Qin, "Effects of thermal treatment on wave velocity as well as porosity and permeability of rock," *Journal-University of Petroleum China Natural Science Edition*, vol. 27, no. 4, pp. 70–72, 2003.

[42] S. U. O. Yu, G. Hong-kui, W. Xiao-qiong, M. Fan-bao, and L. Jun-rong, "Instruments and methods with high-precision for wave velocity measurement on shale debris," *Rock and Soil Mechanics*, vol. 39, no. 1, pp. 385–392, 2018.

[43] J. Zhang, W. B. Standifird, J.-C. Roegiers, and Y. Zhang, "Stress-dependent fluid flow and permeability in fractured media: from lab experiments to engineering applications," *Rock Mechanics and Rock Engineering*, vol. 40, no. 1, pp. 3–21, 2007.